Apolipoprotein M expression increases the size of nascent preβ HDL formed by ATP binding cassette transporter A1

Anny Mulya,[1] Jeongmin Seo, Amanda L. Brown, Abraham K. Gebre, Elena Boudyguina, Gregory S. Shelness, and John S. Parks[2]

Department of Pathology/Section on Lipid Sciences, Wake Forest University Health Sciences, Winston-Salem, NC 27157

Abstract **Apolipoprotein M (apoM) is a novel apolipoprotein that is reportedly necessary for preβ HDL formation; however, its detailed function remains unknown. We investigated the biogenesis and properties of apoM and its effects on the initial steps of nascent preβ HDL assembly by ABCA1 in HEK293 cells. Transiently transfected apoM was localized primarily in the endomembrane compartment. Pulse-chase analyses demonstrated that apoM is inefficiently secreted, relative to human serum albumin, and that ~50% remains membrane-associated after extraction with sodium carbonate, pH 11.5. To investigate the role of apoM in nascent preβ HDL formation, ABCA1-expressing or control cells, transfected with empty vector, apoM, or C-terminal epitope-tagged apoM (apoM-C-FLAG), were incubated with ^{125}I-apoA-I for 24 h. Conditioned media were harvested and fractionated by fast-protein liquid chromatography (FPLC) to monitor HDL particle size. Preβ HDL particles were formed effectively in the absence of apoM expression; however, increased apoM expression stimulated the formation of larger-sized nascent preβ HDLs. Immunoprecipitation with anti-apoA-I antibody followed by apoM Western blot analysis revealed that little secreted apoM was physically associated with preβ HDL. Our results suggest that apoM is an atypical secretory protein that is not necessary for ABCA1-dependent preβ HDL formation but does stimulate the formation of larger-sized preβ HDL. We propose that apoM may function catalytically at an intracellular site to transfer lipid onto preβ HDL during or after their formation by ABCA1.**—Mulya, A., J. Seo, A. L. Brown, A. K. Gebre, E. Boudyguina, G. S. Shelness, and J. S. Parks. **Apolipoprotein M expression increases the size of nascent preβ HDL formed by ATP binding cassette transporter A1.** ***J. Lipid Res.*** **2010.** 51: **514–524.**

Supplementary key words high density lipoprotein biogenesis • high density lipoprotein size • protein secretion

The inverse relationship between plasma HDL cholesterol concentration and the risk of developing premature atherosclerotic vascular disease has generated interest in understanding the role of HDL-associated apolipoproteins on the atheroprotective function of HDL (1–4). The presence of apolipoproteins on HDL plays a major role in the structural organization and intravascular metabolism of HDL, particularly with regard to cellular receptor and transporter binding, lipolytic enzyme activity, and lipid exchange or transfer. Human HDL contains two major apolipoproteins, apolipoprotein A-I (apoA-I) and apoA-II, which represent ~80% and ~20% of the total protein content of HDL particles, respectively (5, 6). In addition, human HDL also contains several other minor apolipoproteins, including apoA-IV (7, 8), the C-apolipoproteins (9, 10), apoD (11), apoE (12), apoJ (13), and apoL (14).

Preβ HDL is a descriptive term to differentiate HDLs on the basis of electrophoretic mobility in agarose gels (15). In normolipidemic human plasma, 90–95% of total HDL is α-migrating HDL, and only 5–10% is preβ HDL (16, 17). Preβ HDLs in human plasma exist as several subpopulations of discrete sizes (18). The formation of preβ HDL is thought to be important for reverse cholesterol transport (RCT), a process by which excess cholesterol in peripheral tissues is transported to the liver for secretion into bile and elimination from the body in feces. Preβ HDLs have been suggested to be the initial acceptors of excess

This work was supported by National Institutes of Health Grants HL-049373 (J.S.P. and G.S.S.), HL-054176 (J.S.P.), and AT027820 (J.S.P.) and American Heart Association Mid-Atlantic Affiliate Predoctoral Fellowship 0515420U (A.M.). Its contents are solely the responsibility of the authors and do not necessarily represent the official views of the National Institutes of Health or other granting agencies.

Manuscript received 11 September 2009 and in revised form 18 September 2009.

Published, JLR Papers in Press, September 11, 2009
DOI 10.1194/jlr.M002162

Abbreviations: apo, apolipoprotein; ER, endoplasmic reticulum; FPLC, fast-protein liquid chromatography; PL, phospholipid; RCT, reverse cholesterol transport; WT, wild type.

[1] Present address of A. Mulya: Department of Cell Biology, Lerner Research Institute, Cleveland Clinic Foundation, Cleveland, OH 44195.

[2] To whom correspondence should be addressed.
e-mail: jparks@wfubmc.edu

cell cholesterol in the first step of RCT and, as such, represent critical intermediates in this process.

In 1999, Xu and Dahlback (19) isolated a novel 26 kDa protein, human apoM, that associates with HDLs. Although apoM is predominantly associated with HDL in plasma, only about 5% of HDL particles contain apoM (20), and an even smaller fraction (0.2–1%) of LDL particles in plasma contain apoM (21). ApoM is reported to have an uncleaved signal peptide that behaves like a hydrophobic signal anchor, resulting in integral association with membranes and lipoproteins (19). Recently, Wolfrum, Poy, and Stoffel (22) demonstrated that the lack of apoM expression in Tcf1α (hepatic nuclear factor 1α)$^{-/-}$ mice or in apoM small interfering RNA-injected mice leads to formation of unusual larger-sized HDL_1 particles and the disappearance of preβ HDL in plasma, suggesting that apoM may play a role in HDL metabolism, particularly with regard to formation or catabolism of preβ HDL.

ABCA1 is critical for nascent preβ HDL formation (23). Interaction of apoA-I with ABCA1 protein on the cell surface promotes the transmembrane transport of cellular phospholipid (PL) and free cholesterol (FC) to assemble with apoA-I, forming nascent HDL (24). ABCA1 activity is necessary and sufficient to generate heterogeneous-sized nascent HDL particles that resemble plasma preβ HDL in size (23, 25–27). Despite the fact that apoM expression influences plasma preβ HDL levels (22), the role of apoM in nascent preβ HDL assembly by ABCA1 is unknown.

The goal of our study was to determine whether apoM affects nascent preβ HDL assembly by ABCA1. To accomplish this, we performed a series of experiments in which nascent preβ HDL formation was investigated during incubation of apoA-I with ABCA1-expressing or control cells transiently transfected with apoM cDNA. We were interested in the degree to which apoM expression affected the size and quantity of nascent preβ HDL and the extent to which apoM associated with nascent HDL. We were also interested in the secretion efficiency of apoM since it has been reported to be an integral membrane protein (19). Our results show that apoM is poorly secreted from HEK293, and only a small fraction of the secreted apoM is associated with nascent HDL. Nevertheless, expression of apoM resulted in a dose-dependent increase in preβ HDL size. Thus, we hypothesized that apoM may function catalytically at an intracellular site to transfer lipid onto nascent preβ HDL during or after their formation by ABCA1.

MATERIALS AND METHODS

Cell culture

Human embryonic kidney 293 Flp-In™ (Control; Invitrogen) and HEK293-ABCA1 cells (a generous gift from Dr. Michael Hayden, University of British Columbia, Canada) were maintained as described previously (23).

Antibodies

Anti-apoM polyclonal antiserum was generated as described by Richter et al. (28). ApoM peptide (amino acids 140–159; GYQRFLLYNRS-PHPPEKCVE) was synthesized (American Peptide, Sunnyvale, CA) and processed to >85% purity, conjugated to keyhole limpet hemocyanin (KLH), and used for immunization of rabbits (Lampire Biological Laboratories, Pipersville, PA). Antiserum was tested by ELISA using the apoM peptide conjugated to BSA as antigen and by Western blotting of medium from apoM-transfected and control cells. Rabbit anti-ABCA1 antiserum was raised to a 24-mer peptide of the C-terminal region of mouse Abca1 conjugated to KLH as previously described (29).

Goat anti-human apoA-I polyclonal antibody was from Biodesign (K45252G), and mouse anti-M2-FLAG monoclonal (F3165) and mouse anti-β-actin monoclonal antibody (A5441) were purchased from Sigma. Rabbit polyclonal anti-GRP94 antibody (ab18055) and AlexaFluor 594-conjugated lectin GS-II antibody (L21416) for endoplasmic reticulum (ER) and Golgi immunodetection were purchased from Abcam and Molecular Probes, respectively. Secondary antibodies for Western blot (anti-mouse horseradish peroxidase) and immunofluorescence (FITC-conjugated anti-mouse/Rhodamine-conjugated anti-rabbit) analysis were from Pierce and Jackson Immunoresearch, respectively.

ApoM-WT and apoM-C-FLAG cDNA cloning into pcDNA3

ApoM cDNA (accession number BC020683) was purchased from the National Institutes of Health mammalian gene collection-human (Invitrogen-iGene, Clone ID 4733993). ApoM-wild type (WT) and apoM-C-FLAG (apoM with C-terminal FLAG epitope tag) cDNAs were produced by PCR amplification using primer combinations as follows: ApoM-WT forward, 5′-CTGCGGATCCTGAAGATGTTCCACCAAATTTGGGCAGCTCTGC-3′; apoM-WT reverse, 5′-GCAGCTACGTCTAGATCAGTTATTGGACAGCTCACAGGCCTCTT-3′; apoM-CFLAG forward, 5′-CTGCGGATCCTGAAGATGTTCCACCAAATTTGGGCAGCTCTGC-3′; and apoM-CFLAG reverse, 5′-TACGTCTAGATCACTTGTCGTCGTCGTCCTTGTAGTCGTTATTGGACAGCTCACAGGCCTCTTGATTC-3′. Oligonucleotide-encoded *Bam*HI and *Xba*I restriction enzyme sites were introduced, respectively, at the 5′ and 3′ flanking sites of the apoM-WT and apoM–C-FLAG cDNAs. Amplified cDNAs were digested with *Bam*HI and *Xba*I and then cloned into the same sites in pcDNA3. Automated DNA sequencing was performed for individual clones of apoM-WT and apoM-C-FLAG pcDNA3 to verify sequence integrity.

Transfection of apoM-WT and apoM-C-FLAG cDNA

Cells were grown on poly-L-lysine HBr (Sigma; P1399)-coated plates until they reached 95% confluence, after which they were transfected for 24 h with empty vector (pcDNA3), apoM-WT (pcDNA3-apoM-WT), and apoM-C-FLAG (pcDNA3-apoM-C-FLAG) using Lipofectamine 2000™ (Invitrogen) according to the manufacturer's instructions.

ApoM Western blotting

Cells were lysed with radioimmuno-precipitation buffer (50 mM Tris, pH 7.6, 150 mM NaCl, 0.25% sodium deoxycholate, 1% Nonidet P-40, and protease inhibitors), and cell protein was measured by the BCA protein assay (Pierce). Thirty micrograms of cell lysate protein was fractionated using 4-20% SDS-PAGE and transferred onto a nitrocellulose membrane (Schleicher and Schuell, Keene, NH) by electroblotting (300 mA, 2 h). Membranes were then blocked with 5% nonfat dry milk and 0.1% Tween 20 in TBS (blocking buffer) overnight at 4°C and then incubated with primary antibody [rabbit preimmune antiserum (1:200), anti-apoM antiserum (1:200), or mouse anti-M2-FLAG antibody (1:1000)], followed by secondary antibody (anti-rabbit or anti-mouse horseradish-peroxidase-labeled IgG; Pierce, #NA934V or NXA931, respectively). For visualization, the Supersignal West Pico

chemiluminescence substrate (Pierce) was used, and the image was captured with a FujiFilm LAS-3000 cold camera.

ApoM cellular location by immunofluorescence

Control and ABCA1-expressing HEK-293 cells were seeded onto Labtek II chamber slides (Nalge Nunc, Rochester, NY) precoated with poly-L-lysine, transfected for 6 h with an expression vector for apoM-C-FLAG, and then incubated for 18 h in serum-free DMEM ± 10 μg apoA-I /ml. Cells were immediately fixed with 3% paraformaldehyde for 10 min at room temperature and immunocytochemically labeled with an indirect or direct procedure in which all incubations, including washes, were performed in blocking solution containing 0.1% saponin and 10% goat serum in PBS. Mouse anti-M2 FLAG antibody, rabbit polyclonal anti-GRP94 antibody (Abcam, Cambridge, MA), and AlexaFluor 594-conjugated lectin GS-II (Molecular Probes) were used at 1:400, 1:200, and 1:500 dilution, respectively. FITC or Cy3-conjugated secondary antibodies (Jackson ImmunoResearch) were used at 1:500 dilution. Confocal images were acquired using a C-apochromat ×63 NA 1.2 water immersion objective mounted on a Zeiss LSM510 confocal laser scanning microscope (Carl Zeiss, Thornwood, NY) equipped with multiple-line argon and HeNe lasers. The FITC fluorophore was excited at 488 nm, and the emitted fluorescence was collected using a 505–530 nm band-pass filter, whereas the Alexa 594 and Cy3 probes were excited at 543 nm, and emission was collected using a 565–615 nm band-pass filter.

Analysis of apoM secretion efficiency

Control and ABCA1-expressing cells were cultured in 100 mm dishes and transiently cotransfected with 12 μg apoM-C-FLAG cDNA and 12 μg albumin cDNA, as described above. Twenty-four hours after transfection, cells were metabolically radiolabeled with 100 μCi/ml [^{35}S]Met/Cys (EasyTag Express protein labeling mix; PerkinElmer Life Sciences) in Met/Cys-deficient DMEM for 30 min followed by chase periods of 0, 0.5, 1, 2, 3, and 4 h. At the end of the chase periods, apoM and albumin from media and cell lysates were immunoprecipitated with anti-FLAG M2 and anti-human albumin antibody, respectively, and fractionated by SDS-PAGE. Dried gels were exposed to a phosphor imager screen. Radioactive gel images were captured with a FujiFilm BAS-5000 Imager, and the intensities were quantified using Multigauge V3.0 (FujiFilm). Data were presented as percentage of band intensity at each time point relative to cells at the beginning of the chase (i.e., 0 h time point).

Sodium carbonate extraction of postnuclear membrane

For sodium carbonate extraction (30, 31), control and ABCA1-expressing cells were cotransfected with human albumin and either apoM-C-FLAG or human CD4-N-FLAG (integral membrane protein, N-terminus FLAG) cDNA (31). Twenty-four hours after transfection, cells were radiolabeled with ^{35}S-Met/Cys for 4 h, after which postnuclear membranes were isolated as described (31). The membrane pellet was then resuspended in membrane buffer (10 mM HEPES, pH 7.4, 250 mM sucrose, 10 mM NaCl, 10 mM KCl, 2.5 mM $CaCl_2$, and 2.5 mM $MgCl_2$ plus protease inhibitors), dounce homogenized and adjusted to 0.1 M sodium carbonate, pH 11.5. After incubation on ice for 1 h, the membranes were centrifuged at 240,000 *g* for 30 min in a TLA100.3 rotor. The supernatant was recovered and the pellet was resuspended in an additional 2 ml of 0.1 M sodium carbonate. After incubation and recentrifugation, the pellet fraction was washed twice with 1 ml of TBS and then resuspended in 200 μl of 25 mM Tris HCl, pH 7.4, and 1% SDS. The pellet fraction was boiled for 10 min, cooled to room temperature, and diluted with 800 μl of Triton lysis buffer (0.15 M NaCl, 25 mM Tris HCl, pH 7.5, and 1% Triton X-100). The supernatant fractions were adjusted to the following immunoprecipitation conditions: 50 mM Tris-HCl, pH 7.4, 200 mM NaCl, 70 mM Na_2CO_3, 1 mM $CaCl_2$, and 1% Triton X-100. The final pH was adjusted to 7.2 by adding a predetermined amount of dilute HCl. Both supernatant and pellet fractions were adjusted to 1 mg/ml BSA, 1 mM PMSF, 10 μg/ml leupeptin, and 10 μg/ml pepstatin. Immunoprecipitation with anti-M2-FLAG monoclonal antibody or anti-human albumin antiserum was performed, immunoprecipitates were fractionated on 4–20% SDS PAGE gels, and gels were visualized using a phosphor imager.

Nascent preβ HDL analysis and isolation by size-exclusion chromatography

Control and ABCA1-expressing cells were grown in 3 × 100 mm dishes until they reached 95% confluence and then transfected with empty vector (pcDNA3), apoM-WT, or apoM-C-FLAG for 24 h. The transfection media were then removed and cells were incubated with 10 μg/ml of ^{125}I-apoA-I (10^5 cpm/μg) for 24 h. Immediately prior to incubation, ^{125}I-apoA-I was heated to 60°C (i.e., just above the transition temperature of apoA-I) (32, 33) for 30 min and then cooled to room temperature to standardize the conformational state of apoA-I. After incubation, the conditioned media were harvested and concentrated using an Amicon Ultra-10 concentrator and fractionated on three Superdex-200HR fast-protein liquid chromatography (FPLC) columns (Amersham Biosciences) connected in series using 0.15 M NaCl and 0.01% EDTA, pH 7.4 (column buffer). The particles were eluted at a flow rate of 0.3 ml/min; individual fractions were analyzed for ^{125}I radioactivity, and the ^{125}I profile was plotted. Aliquots of selected fractions were resolved by 4–30% nondenaturing gradient gel electrophoresis and visualized with a phosphor imager to determine the elution position of homogeneously-sized preβ HDL particles, which were then pooled and used for subsequent studies. Our previous work has shown that at least four subfractions of nascent preβ HDL can be isolated by this procedure; we have designated these as preβ 1, 2, 3, and 4 HDL to denote particles of increasing diameter on nondenaturing gradient gel electrophoresis (23).

To determine whether secreted apoM affected nascent preβ HDL assembly, we performed the following experiment. Control cells were plated and transfected either with empty vector, apoM-WT, or apoM-C-FLAG for 24 h. Transfection media were then removed and cells were incubated with DMEM in the presence of 2 mM L-glutamine, 100 units/ml penicillin, and 100 μg/ml streptomycin (DMEM) for 24 h. Conditioned media were then harvested from each treatment, and 10 μg/ml of ^{125}I-apoA-I (10^5 cpm/μg) was added. These media were then used for incubation with nontransfected control and ABCA1-expressing cells for 24 h. After incubation, media were harvested, concentrated, and fractionated using Superdex-200HR columns as described above, and ^{125}I radioactivity profiles were plotted and compared.

In other experiments, empty vector, apoM-WT, and apoM-C-FLAG transfected-control and ABCA1-expressing cells were radiolabeled with 2 μCi/ml of 1α,2α-[^{3}H] cholesterol or [methyl-^{3}H] choline chloride for 16 h and then incubated with 10 μg/ml of nonradiolabeled apoA-I for 24 h. After incubation, conditioned media were concentrated and fractionated by Superdex 200HR FPLC as described above. One hundred microliters of each fraction was quantified for ^{3}H-radioactivity. The ^{3}H-radioactivity profile was plotted and compared with the ^{125}I-radioactivity profile.

Coimmunoprecipitation of apoA-I and apoM on nascent preβ HDL

Nascent preβ1, 2, 3, and 4 HDLs were isolated from media of apoM-C-FLAG-transfected control and ABCA1-expressing cells as described above. One microgram of apoA-I from each nascent

preβ HDL subfraction was immunoprecipitated with goat anti-human apoA-I antibody overnight at 4°C. Protein G Sepharose beads were added to each sample and incubated at 4°C for 1.5 h, after which samples were spun at 12,000 *g* for 10 s to pellet the beads. The supernatant was collected, and proteins in the supernatant were precipitated with TCA. The pelleted Protein G Sepharose beads were washed three times with Triton lysis buffer (0.15 M NaCl, 25 mM Tris HCl, pH 7.5, and 1% Triton X-100) and then boiled for 5 min with immunoprecipitation buffer (0.1% SDS, 10 mM Tris HCl, pH 7.5, and 25 mM EDTA) to recover anti-apoA-I bound protein. The protein recovered from the Protein G Sepharose beads as well as the TCA-precipitated supernatant proteins were resolved using 4–20% SDS-PAGE and transferred to nitrocellulose membranes for Western blot analysis. An aliquot of each preβ HDL fraction equivalent to 1 μg apoA-I was also subjected to TCA precipitation and analyzed on the gels with the supernatant and pellet fractions from the immunoprecipitation. Membranes were incubated with anti-M2-FLAG antibody and anti-mouse IgG peroxidase, and apoM was detected with chemiluminescence substrate (Pierce). Membranes were also exposed to a phosphor imager screen to visualize the ^{125}I radioactivity. Pixel intensities were measured using MultiGauge V3.0 software (FujiFilm).

RESULTS

ApoM expression in control and ABCA1-expressing cells

ApoM expression was investigated by Western blot analysis using control and stably transfected ABCA1-expressing cells transiently transfected with empty vector (pcDNA3), apoM-WT, or apoM-C-FLAG cDNA. Western blot analysis using anti-apoM antisera and anti-M2-FLAG antibody validated the presence of apoM protein in apoM-WT and apoM-C-FLAG transfected cells, but not in pcDNA3-transfected cells (**Fig. 1A**, B). Western blots using preimmune serum showed no evidence of immunoreactivity in the size range of apoM (~26 kDa) (data not shown).

ApoM has been reported to be an integral membrane protein because it retains its hydrophobic signal peptide, which may act as a membrane anchor. We investigated the cellular location of apoM protein in control and ABCA1-expressing transfected cells using immunofluorescence microscopy. Control and ABCA1-expressing cells were transfected with pcDNA3 or apoM-C-FLAG, and immunofluorescence was detected by incubating fixed cells with monoclonal antibody to the FLAG epitope, followed by goat anti-mouse IgG FITC-labeled secondary antibody. We did not detect apoM protein expression in cells transfected with pcDNA3 (data not shown). However, apoM-C-FLAG-transfected cells showed significant expression of apoM protein both in control (data not shown) and ABCA1-expressing cells (**Fig. 2**, left panel). To determine the cellular compartmentalization of apoM protein, colocalization of apoM with ER and Golgi markers was performed (Fig. 2, center and right panels). ApoM was observed predominantly in the exocytic compartments of the cell, as evidenced by the extensive colocalization with GRP94 (ER, top panel) and Lectin GS-II (Golgi, bottom panel). A similar pattern of apoM cellular localization was observed in control cells not expressing ABCA1 (data not shown). No discernible surface

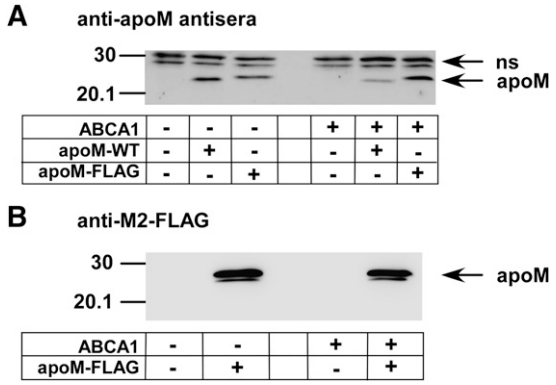

Fig. 1. ApoM protein expression in control and ABCA1-expressing cells. Control and ABCA1-expressing cells were transfected with pcDNA3 (control), apoM-WT, or apoM-C-FLAG cDNA as described in Materials and Methods. Cells were suspended in radioimmunoprecipitation buffer, and 30 μg of cellular protein were fractionated by SDS-PAGE and transferred to nitrocellulose for Western blot analysis. The blots were incubated with rabbit anti-apoM antisera (1:200 dilution) or anti-M2-FLAG antibody (10 μg/ml) as denoted in A and B. Lanes corresponding to control (-ABCA1) and ABCA1-expressing (+) cells transfected with apoM-WT and apoM-FLAG are indicated beneath each gel. Molecular weight (kDa) of protein markers are indicated on the left side of the gels. Arrow indicates migration position of apoM. ns, nonspecific band.

expression of apoM was observed regardless of whether apoA-I was present in the medium or whether ABCA1 was expressed (i.e., control versus ABCA1-expressing cells).

ApoM secretion efficiency in control and ABCA1-expressing cells

To determine whether apoM is secreted into the medium, and whether ABCA1 expression affects its secretion efficiency, we performed pulse-chase metabolic radiolabeling experiments. ABCA1-expressing cells were cotransfected with albumin and apoM-C-FLAG cDNA. Cells were radiolabeled with ^{35}S-Met/Cys for 30 min, followed by chase periods up to 4 h. At the end of each chase period, cell lysate and media were harvested and subjected to immunoprecipitation with anti-human albumin and anti-FLAG antibodies. Compared with albumin, apoM was secreted with slow kinetics and poor efficiency (**Fig. 3**). In ABCA1-expressing cells, ~90% of the initial albumin radiolabel was secreted 1.5 h postchase. In contrast, even after a 4 h chase period, only ~25% of apoM was secreted into the medium. Further, while albumin recovery was 100% after 4 h, only ~50% of apoM was recovered, indicating a substantial degree of intracellular degradation. In a separate experiment, 4 h conditioned media and cell lysate from apoM-C-FLAG transfected ABCA1-expressing cells were analyzed with Western blotting using an anti-FLAG antibody to monitor apoM mass distribution. Less than 20% of total apoM mass was recovered in media (data not shown), supporting the pulse-chase kinetic results and suggesting that very little expressed apoM undergoes secretion.

Sodium-carbonate extractability of apoM

To further investigate whether a fraction of apoM has properties of an integral membrane protein, microsomes

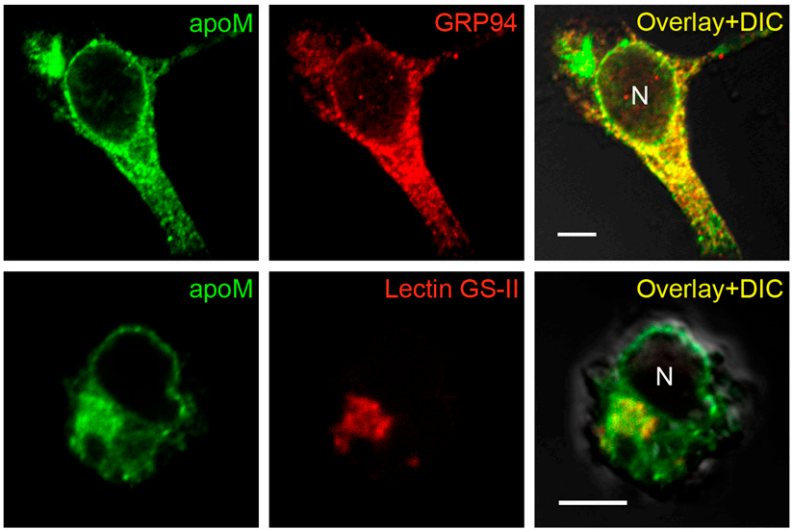

Fig. 2. Subcellular localization of apoM in ABCA1-expressing cells. ABCA1-expressing cells were transiently transfected with apoM-C-FLAG expression vector and visualized by confocal fluorescence microscopy following immunolabeling with anti-FLAG antibodies (apoM, green), anti-GRP94 antibody (upper panel; ER marker, red), or lectin GS-II (lower panel; Golgi marker, red) as described in Materials and Methods. In the right panels, composite fluorescent signals (1 μm confocal slices) were superimposed on Nomarski differential interference contrast (DIC) images. Note the extensive colocalization (yellow) and the absence of apoM immunoreactivity at the plasma membrane. N, nucleus. Bars = 5 μm.

from cells transfected with apoM-C-FLAG, albumin, or CD4-N-FLAG cDNA were subjected to extraction with 0.1 M sodium carbonate, pH 11.5 (30, 34). Supernatants from two sequential carbonate extractions and the final membrane pellets were subjected to immunoprecipitation with anti-FLAG or anti-human albumin antibody. The immunoprecipitated proteins were fractionated by SDS-PAGE and visualized using a phosphor imager (**Fig. 4**). As expected, ~80% of albumin, a known soluble secretory protein, was efficiently extracted with two sequential rounds of sodium carbonate, with ~20% remaining in the membrane pellet (P). In contrast, CD4-N-FLAG, an integral membrane protein, was resistant to carbonate extraction and was recovered almost exclusively in the membrane pellet. ApoM protein extractability was intermediate to that of a secretory protein (albumin) and an integral membrane protein (CD4-N-FLAG), as shown by the nearly equal band intensities in the supernatant (S) and membrane pellet (P) fractions. It is also of interest that, unlike albumin, the apoM not removed from the microsomes after the first extraction remained stably associated with membranes, as evidenced by its complete absence in the S2 fraction.

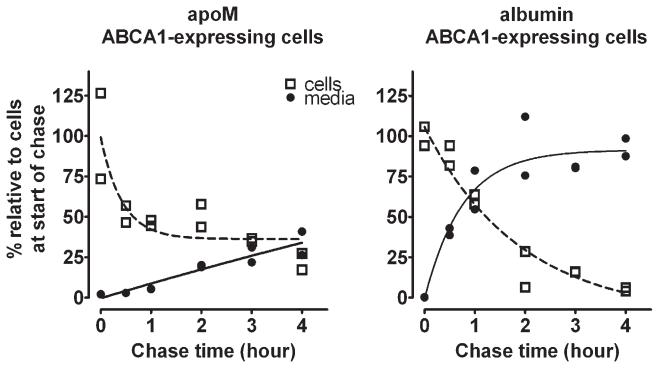

Fig. 3. Secretion efficiency of apoM and albumin from HEK293 ABCA1-expressing cells. HEK293 ABCA1-expressing cells were cotransfected with human albumin and apoM-C-FLAG cDNA, followed by a 30 min pulse with ^{35}S-Cys/Met and chase periods up to 4 h. Albumin and apoM were immunoprecipitated from chase media and cell lysates and separated on 4–20% SDS PAGE gels. The gels were dried and apoM and albumin band intensities were quantified using a phosphor imager. Data (duplicate values at each time point) are plotted as percentage of intensity relative to cells at the start of the chase period; the line of best fit was determined by curve fitting using GraphPad Prism software.

ApoM expression results in larger-sized nascent HDL particle formation by ABCA1

We previously demonstrated that interaction of apoA-I with ABCA1-expressing cells leads to the formation of heterogeneous-sized nascent preβ HDL particles that can be isolated preparatively by size-exclusion FPLC (23). To determine whether apoM expression plays a role in nascent preβ HDL particle formation and influences the size distribution of nascent preβ HDL particles, we transfected control and ABCA1-expressing cells with empty vector, apoM-WT, and apoM-CFLAG cDNA and incubated the cells in the presence of ^{125}I-apoA-I for 24 h. Conditioned media were harvested and fractionated by size-exclusion FPLC. Incubation of ^{125}I-apoA-I with control cells (**Fig. 5A**,

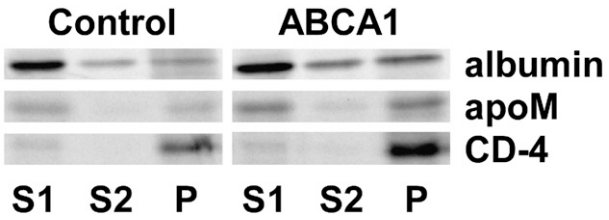

Fig. 4. Extraction of post nuclear membranes of HEK293 control and ABCA1-expressing cells with sodium carbonate, pH 11.5. Control or ABCA1-expressing HEK293 cells were transiently transfected with albumin, apoM-C-FLAG (apoM), or CD-4-N-FLAG (CD-4) cDNA, as indicated on the right side of the figure. Microsomal membranes prepared from the transfected cells were subjected to two rounds of extraction with 0.1 M sodium carbonate, pH 11.5. The protein contained in the supernatant from the first (S1) and second (S2) carbonate extraction as well as the final membrane pellet (P) were immunoprecipitated with anti-human albumin or -FLAG antibody. Immunoprecipitates were fractionated by 4–20% SDS-PAGE and proteins visualized with a phosphor imager.

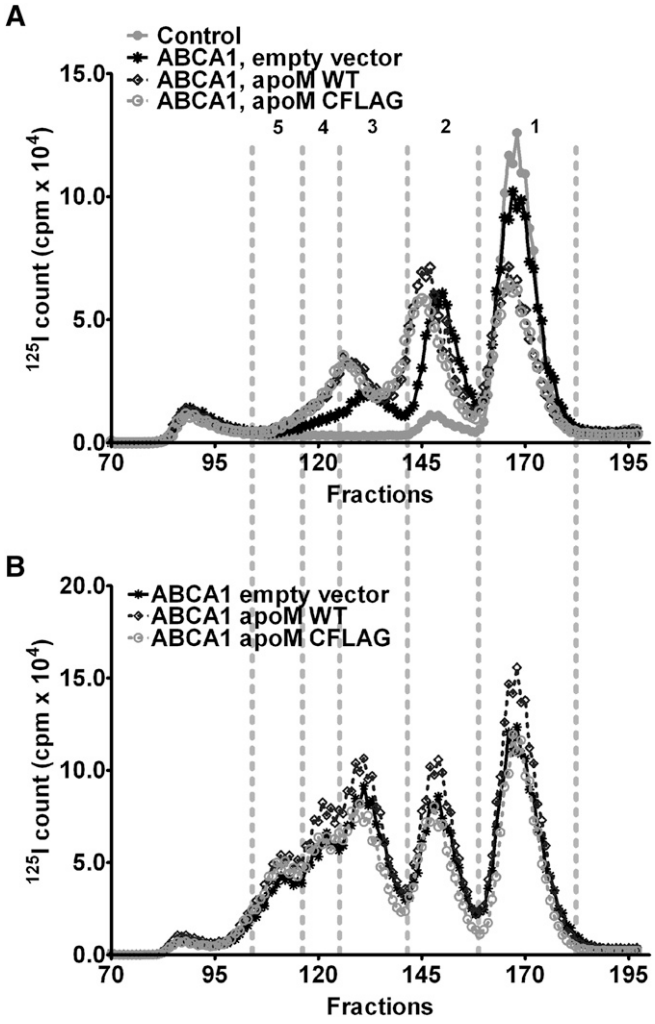

Fig. 5. Cellular apoM expression results in larger-sized nascent HDL particles A: Nascent HDL distribution of conditioned medium of control and ABCA1-expressing cells transfected with empty vector, apoM-WT, or apoM-C-FLAG, followed by 24 h incubation with ^{125}I-apoA-I. Experimental details are provided in Materials and Methods. B: Nascent HDL distribution in apoM conditioned medium after incubation with ^{125}I-apoA-I and ABCA1-expressing cells. Control cells (i.e., no ABCA1 expression) were transfected with empty vector, apoM-WT, or apoM-C-FLAG cDNA for 24 h. The transfection medium was removed and replaced with fresh medium for another 24 h incubation to generate apoM conditioned medium. The apoM conditioned medium was then added along with ^{125}I-apoA-I to cells expressing ABCA1, but not apoM. After an additional 24 h incubation, the medium was harvested, concentrated, and fractionated by high resolution FPLC. The dashed lines denote the elution ranges of preβ1(<7.1 nm), 2 (7.4–7.5 nm), 3 (9.7–10.4 nm), 4 (11.8–12.6 nm), and 5 (>12.6 nm) HDL for ABCA1-expressing cells in the absence of apoM expression (i.e., empty vector transfected).

control) or with control cells transfected with empty vector, apoM-WT, or apoM-C-FLAG did not lead to formation of nascent preβ HDL particles (data not shown). These results agree with our previous study that showed no detectable nascent preβ HDL formation in the absence of ABCA1 expression (23). Incubation of ^{125}I-apoA-I with empty vector (pcDNA3)-transfected ABCA1-expressing cells initiated formation of heterogeneous-sized nascent preβ HDL, similar to our previously published observations (Fig. 5A, ABCA1, empty vector) (23). Transfection of ABCA1-expressing cells with apoM-WT and apoM-C-FLAG cDNA resulted in less radiolabeled apoA-I in the smallest particle elution region of the column (i.e., preβ1 HDL; fractions 162–175) and an increase in formation of larger-sized nascent preβ2, preβ3, and preβ4 HDL that were eluted in earlier fractions (Fig. 5A).

To investigate whether the formation of larger-sized nascent preβ HDL particles observed with apoM expression occurred exclusively due to interactions in the medium, apoM-conditioned medium from control cells (not expressing ABCA1) was added along with ^{125}I-apoA-I to cells expressing ABCA1, but not apoM. Figure 5B shows a similar distribution of nascent preβ HDL particles for conditioned media derived from pcDNA3, apoM-WT, and apoM-C-FLAG cDNA-transfected cells, demonstrating that apoM-conditioned media alone is not sufficient to promote the formation of larger preβ HDL particles as observed in Fig. 5A, where cells were transfected with apoM. These results suggest that the formation of larger-sized nascent preβ HDL upon expression of apoM may occur at an intracellular site and/or at the cell surface during nascent HDL particle assembly by ABCA1.

ApoM expression redistributes ^{3}H-cholesterol and ^{3}H-PL to larger-sized nascent HDL particles

As shown in Fig. 5A, apoM expression resulted in a shift in elution of ^{125}I-apoA-I to larger nascent HDL particles. We next investigated whether expression of apoM would affect the distribution of ^{3}H-cholesterol and ^{3}H-PL among nascent HDL particles. **Figure 6** shows the ^{3}H-cholesterol and ^{3}H-choline-containing PL elution profile of conditioned media obtained from ABCA1-expressing cells transfected with pcDNA3 (empty vector), apoM-WT, or apoM-C-FLAG cDNA. The elution profile of ^{125}I-apoA-I in the different-sized nascent HDL particles, determined in a separate experiment, is denoted by the vertical dashed lines. Similar to results for ^{125}I-apoA-I (Fig. 5A), the elution profiles of ^{3}H-PL (Fig. 6A) and ^{3}H-cholesterol (Fig. 6B) were shifted to larger particle sizes when apoM was expressed by cells. The increase in radioactivity of ^{3}H-PL in preβ 3–5 HDL with apoM expression was less striking than that of ^{3}H-cholesterol, presumably due to a greater dilution of ^{3}H-choline specific activity in cells relative to that of ^{3}H-cholesterol.

Increase in nascent HDL particle size is related to apoM expression level

Next, we examined whether there is a dose-dependent relationship between apoM expression and the particle size of nascent HDL formed by ABCA1. Transfection of ABCA1-expressing cells with increasing amounts of apoM-C-FLAG expression vector resulted in a proportional increase in cellular apoM protein expression (**Fig. 7A**). This DNA dose-dependent increase in apoM protein level was accompanied by a stepwise shift of the FPLC elution profile of nascent preβ HDL particles to earlier elution fractions (Fig. 7B, C), indicative of increasing particle size. Analysis of the nascent HDL peak shift as a function of

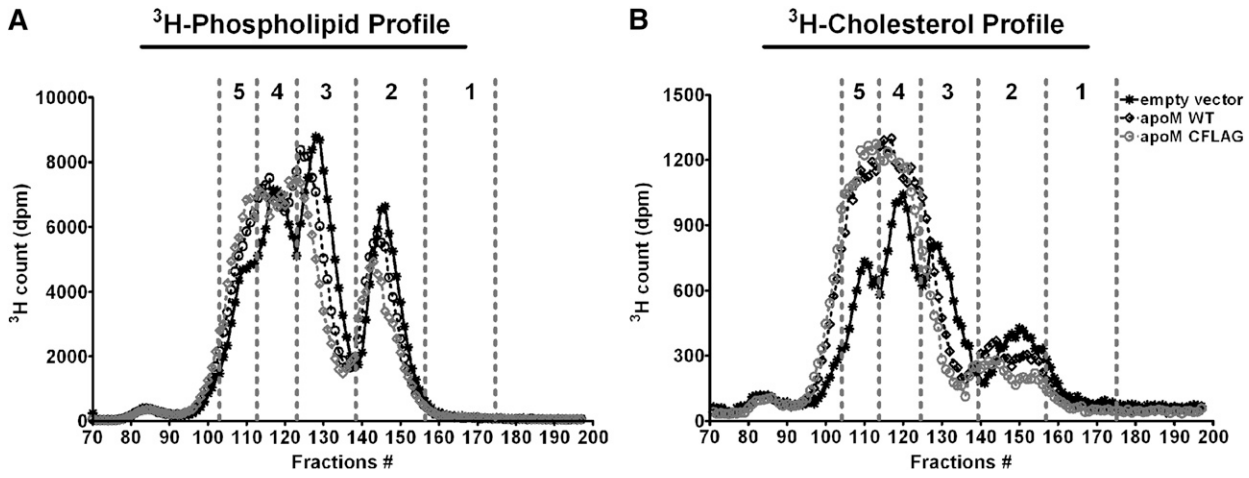

Fig. 6. Cellular apoM expression results in a shift of nascent HDL PL and cholesterol to larger-sized nascent HDL particles. ABCA1-expressing cells were transfected with empty vector, apoM WT or apoM C-FLAG and radiolabeled overnight with either ^{3}H-choline chloride or ^{3}H-cholesterol, followed by incubation with 10 μg/ml of apoA-I for 24 h. Conditioned media were harvested, concentrated, and fractionated by high resolution FPLC. Radiolabels in each fraction were determined by liquid scintillation counting. The dashed lines denote the elution ranges of preβ1-5 HDL for ABCA1-expressing cells in the absence of apoM expression (i.e., empty vector transfected). A: ^{3}H-choline- PL elution profile, and (B) ^{3}H-cholesterol elution profile.

apoM expression suggested that the increase in HDL size was more pronounced with larger nascent HDL species (≥preβ3) than smaller preβ2 HDL (Fig. 7D).

apoM associates poorly with apoA-I containing nascent HDL particles

The ABCA1-mediated formation of larger-sized nascent preβ HDL particles with apoM expression could result from the association of apoM with nascent preβ HDL particles. To investigate this possibility, we performed coimmunoprecipitation experiments using anti-FLAG, anti-apoA-I, and anti-apoM antisera with preβ HDL particles isolated from the media of apoM-C-FLAG-transfected ABCA1-expressing cells incubated in the presence of ^{125}I-apoA-I. Immunoprecipitation of isolated nascent preβ HDL particles with anti-FLAG antibody did not result in detectable apoA-I in the precipitate by Western blot analysis and ^{125}I-radioactivity detection (data not shown). In addition, immunoprecipitation of isolated nascent preβ HDL particles with anti-apoA-I antibody followed by anti-FLAG Western blot analysis demonstrated that most of the secreted apoM did not coimmunoprecipitate (P) with apoA-I-containing nascent preβ HDL particles (**Fig. 8A**) and remained in the supernatant (S) fraction. The phosphor imager results showed that little ^{125}I-apoA-I remained in the supernatant fraction after immunoprecipitation (Fig. 8B). These results suggest that most of the apoM that was secreted into the media was not associated with nascent preβ HDL particles.

DISCUSSION

The goal of this study was to investigate the role of apoM expression on the initial steps of nascent preβ HDL particle assembly by ABCA1 in the absence of other HDL-modifying proteins. To accomplish this, we investigated nascent HDL particle formation by transient transfection of apoM cDNA into HEK293 cells expressing ABCA1 or control cells not expressing ABCA1. We have previously shown that HEK293 cells lack expression of other known HDL-modifying proteins (23). The results of our study provide several novel observations. First, apoM expression is not necessary for the formation of nascent HDL by ABCA1; however, apoM expression leads to formation of larger-sized nascent preβ HDL particles. Furthermore, the formation of the larger-sized nascent preβ HDL particles upon apoM expression appears to occur at the expense of smaller preβ1 HDL fractions, perhaps by fusion or transfer of apoA-I, cholesterol, and PL from smaller to larger nascent preβ HDL (Figs. 5 and 6). Second, apoM was poorly secreted relative to albumin (Fig. 3) and appears to be retained in intracellular compartments, such as the ER and Golgi (Figs. 2 and 4). Third, of the <20% of apoM that is secreted, <3% is associated with newly assembled nascent preβ HDL particles (Fig. 8). Finally, the presence of apoM in media of cells expressing ABCA1 is not sufficient to facilitate the conversion of small preβ HDL to larger preβ HDL, suggesting that this conversion occurs within the cell. Thus, we hypothesize that apoM may function at an intracellular site to facilitate the transfer of cholesterol, PL, and apoA-I onto nascent preβ HDL particles during or after their formation by ABCA1.

Wolfrum, Poy, and Stoffel (22) showed that reduction of apoM expression in hepatocytes from hepatic nuclear factor $1\alpha^{-/-}$ mice or mice treated with apoM small interfering RNA resulted in the disappearance of preβ HDLs in the circulation and that treatment of hepatic nuclear factor $1\alpha^{-/-}$ mice with apoM-adenovirus resulted in the reappearance of preβ HDL particles in plasma. These results suggested that apoM expression was critical for preβ HDL formation in vivo. Furthermore, loss of apoM expression resulted in the accumulation of large HDL_1 particles in plasma and an increase in plasma turnover of HDL_2 particles, suggesting that apoM also affected the metabolism of

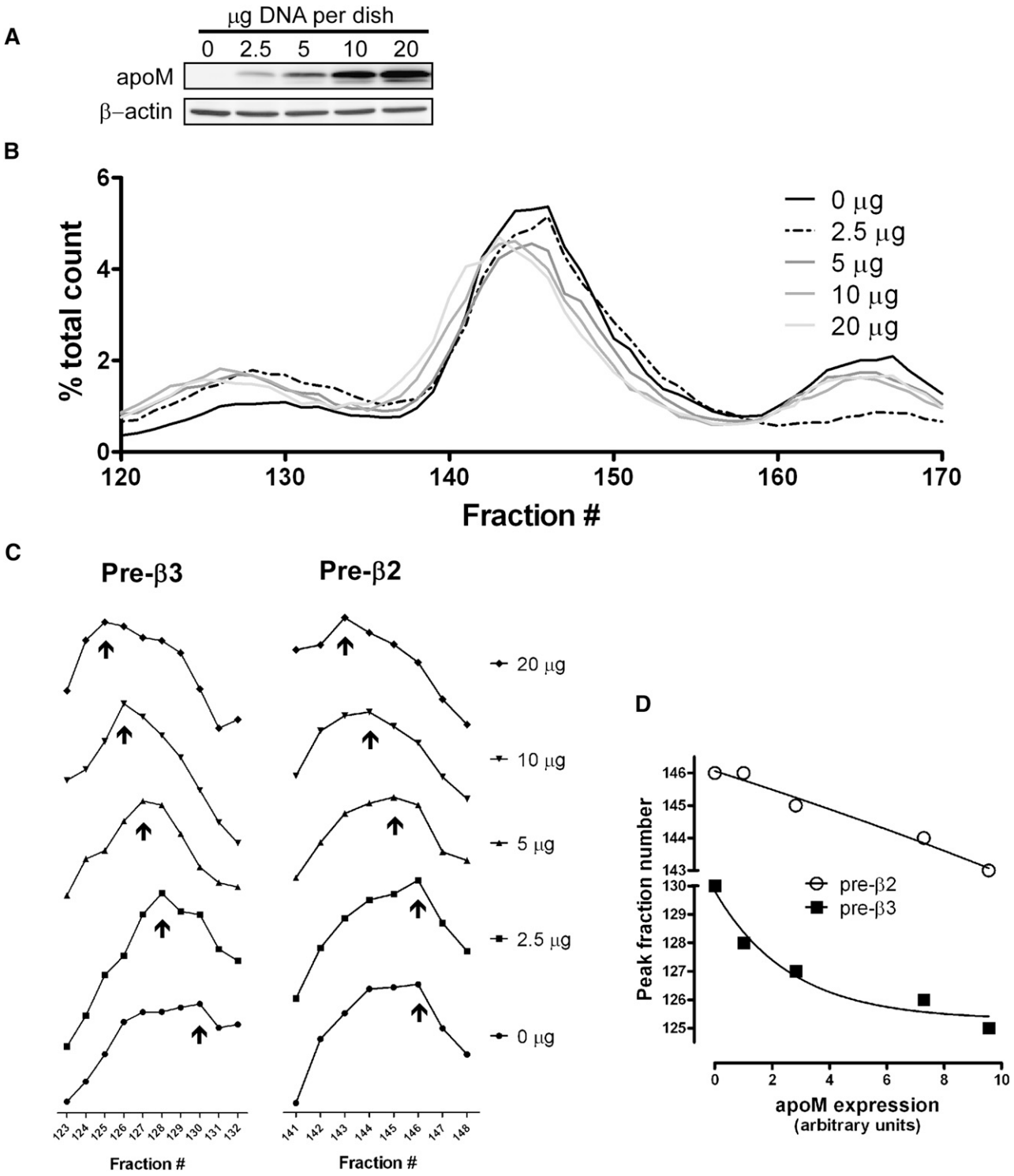

Fig. 7. Increase in nascent HDL particle size increases with apoM expression. ABCA1-expressing cells in 100 mm dishes were transiently transfected with varying amounts (0–20 μg) of apoM-C-FLAG expression vector and empty vector (total 20 μg DNA per dish) and then incubated with ^{125}I-apoA-I for 24 h. A: DNA dose-dependent apoM protein expression in ABCA1-expressing cells, determined by Western blot analysis with β-actin as load control. B: Conditioned media from the apoM transfections were concentrated and fractionated by high resolution FPLC as in Fig. 5. C: Preβ 2 and 3 regions for each transfection in B were replotted with vertical expansion and displacement for comparison purposes. Arrows denote peak preβ 2 and 3 fractions for each transfection. D: Peak elution positions of preβ2 and preβ3 on size exclusion column (C; denoted by arrows) are plotted against apoM protein expression levels quantified from Western blot analysis (A). The lines of best fit were determined by curve fitting using GraphPad Prism software.

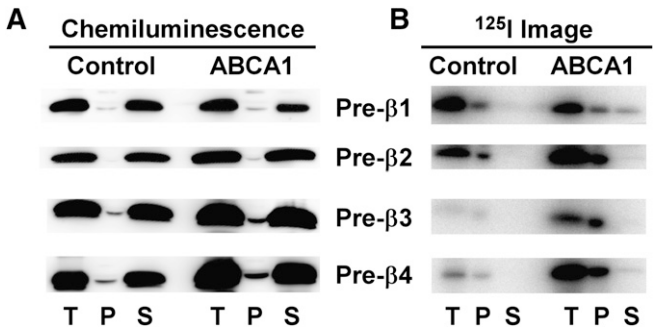

Fig. 8. Analysis of apoM association with nascent preβ HDL particles. Control and ABCA1-expressing cells were transfected with apoM-C-FLAG cDNA and incubated with ^{125}I-apoA-I for 24 h. Conditioned media were concentrated and fractionated by high-resolution FPLC, and nascent preβ1 to 4 HDL particles were isolated. Each preβ HDL fraction (1 μg apoA-I) was subjected to TCA precipitation (i.e., total protein) or immunoprecipitation with goat anti-human apoA-I antibody. The pellet and supernatant fractions from immunoprecipitation and the TCA precipitated total protein were fractionated by 4–20% SDS-PAGE. Proteins on the gels were transferred to a nitrocellulose membrane and incubated with anti-M2-FLAG antibody and anti-mouse horseradish-peroxidase-labeled IgG (1:10,000), followed by incubation with chemiluminescence reagent (A). ^{125}I-apoA-I on the blot was visualized using a phosphor imager (B). T, P, and S, total protein, pellet, and supernatant fractions, respectively.

plasma HDL particles. However, another recent study in which human apoM expression was increased in transgenic mice or eliminated in gene-targeted mice found that apoM expression had no effect on plasma preβ HDL levels and HDL particle size and small effects (~10–20%) on plasma HDL concentrations (35). The reason for these discrepant results may be related to methodological differences and the possibility that deletion of hepatic nuclear factor 1α may exert additional effects besides elimination of apoM expression.

Our study is the first to specifically address the role of apoM in the assembly of nascent HDL particles by ABCA1 and demonstrates that apoM is not necessary for preβ HDL formation. However, we did observe that apoM expression facilitates the formation of larger preβ HDL by ABCA1. Using HEK293 cells that do not express apoM (23), we have isolated four distinct-sized subfractions of preβ HDL assembled by ABCA1 in the presence of apoA-I. Transient transfection of both native and FLAG-tagged apoM cDNA results in a shift in the size distribution of preβ HDL, with an increase in larger preβ HDL particles due to increased incorporation of apoA-I, cholesterol, and PL from smaller preβ HDL to larger preβ particles (Figs. 5, 6). Whether apoM functions in the transfer of lipid from smaller to larger preβ HDL particles or catalyzes the fusion of smaller HDL particles to generate larger nascent HDL is not known. Several studies suggest that apoM may be involved in HDL particle remodeling (22, 35). For instance, apoM may function to remodel HDL_2 particles in plasma, resulting in the formation of preβ HDL. Incubation of plasma from apoM transgenic mice resulted in increased preβ HDL, perhaps secondary to increased expression of PL transfer protein (35). In the absence of this apoM-facilitated remodeling, there may be an accumulation of abnormally large HDL in plasma, such as the HDL_1 particles described by Wolfrum, Poy, and Stoffel (22). ApoM is a member of the lipocalin gene family, contains a predicted hydrophobic pocket, and binds retinol and retinoic acid. Ahnstrom et al. (36) reported that apoM does not bind cholesterol, fatty acids, or prostaglandins, suggesting that apoM may not remodel HDL particles by directly transferring lipid. However, these studies were performed with mutant constructs of apoM that lacked the signal peptide, which may alter its function. Further studies will be necessary to determine the exact role of apoM in nascent HDL particle assembly.

The increase in preβ HDL particle size with apoM expression may require a direct protein-protein or protein-lipid interaction. However, immunoprecipitation of apoA-I followed by apoM Western blot analysis of isolated nascent preβ HDL particles demonstrated that only a small fraction (<3%) of the secreted apoM was associated with newly assembled apoA-I-containing nascent preβ HDL particles (Fig. 8), suggesting that if extensive interaction occurs, it is transient or easily disrupted. Nonetheless, of the small interacting pool, there was an increase in apoM content as preβ HDL particle size increased (Fig. 8), which may indicate a preference for apoM associating with more cholesterol-enriched preβ HDL particles (23). These results agree with a study reporting that, although apoM associates mainly with HDL particles in plasma, only 5% of HDL particles in human plasma contained apoM. Furthermore, plasma HDL containing apoM had increased free cholesterol content compared with HDL particles with no apoM (20).

It is likely that apoM functions to increase preβ HDL particle size at an intracellular site. Consistent with this prediction, apoM is poorly secreted from HEK293 cells (Fig. 3) and is retained in intracellular compartments (Figs. 2 and 3), suggesting limited or no distribution of apoM on the plasma membrane of HEK293 cells. Using pulse-chase and immunoprecipitation procedures, we show that <20–25% of newly synthesized apoM was secreted from apoM-transfected HEK293 cells after 4 h (Fig. 3). In contrast, almost 90% of newly synthesized albumin was secreted after just a 1.5 h chase. ApoA-I, the major apolipoprotein on HDL particles, has a secretion efficiency of 95% and 65% from hepatic and apoA-I-transfected non-hepatic cell lines, respectively (37). These results suggest a possible explanation for the considerable difference in apoM (2–15 mg/dl) (38) and apoA-I (100–125 mg/dl) (5, 39–42) concentration in human plasma. Low secretion efficiency of apoM may be related to the retention of its N-terminal signal peptide in the mature protein, which is hydrophobic, and may target apoM for membrane association, as suggested by Xu and Dahlback (19). In support of this prediction, we also observed that some apoM was resistant to alkaline carbonate extraction (Fig. 4), suggesting that a pool of apoM may have properties of an integral membrane protein, similar to the CD4-N-FLAG integral membrane protein control. Furthermore, incubation of apoM-conditioned media from control cells was not suffi-

cient to facilitate the conversion of small preβ HDL to larger preβ HDL when added with apoA-I to ABCA1-expressing cells (Fig. 5B). These results, taken together, suggest that the apoM-mediated increase in preβ HDL particle size occurred at an intracellular site.

HDL particle assembly occurs at the plasma membrane and in endosomal compartments of the cell, but the quantitative significance of intracellular assembly of HDL in endosomes is unclear (43–47). A small percentage of apoA-I lipidation occurs within the secretory pathway of cells that secrete apoA-I, such as hepatocytes or hepatoma cell lines (48, 49). However, HEK-293 cells do not secrete apoA-I, so the only source of apoA-I available for HDL particle assembly in our experiments is that which is added to the medium. Based on our combined results, we hypothesize that apoM may facilitate lipid addition by ABCA1 during intracellular nascent HDL particle formation and/or facilitate nascent HDL particle fusion as apoA-I recycles through the endosomal compartment, resulting in appearance of larger preβ HDL particles in the medium.

Our previous work has shown that the initial interaction of apoA-I with ABCA1 in vitro predetermines the in vivo catabolism of preβ HDL particles (50). In that study, we observed a significant trend of increased liver and decreased kidney catabolism with increasing nascent preβ HDL particle size. In the context of RCT, any circumstance that increases the capacity of preβ HDL to accept cellular cholesterol and/or direct catabolism of the preβ HDL particle toward the liver should increase the efficiency of RCT, since liver uptake and transport of cholesterol into the bile are distal steps in RCT. If our in vitro results can be extrapolated to preβ HDL physiology in vivo, apoM may facilitate RCT by conversion of small preβ HDL into larger preβ HDL, resulting in a greater proportion of HDL that are ultimately taken up by the liver, resulting in more cholesterol transport into the terminal steps of RCT.

The authors thank Dr. Michael Hayden from the University of British Columbia, Vancouver, Canada for providing us with ABCA1-expressing cells. The authors gratefully acknowledge Karen Klein (Research Support Core, Wake Forest University Health Sciences) for editing the manuscript.

REFERENCES

1. Gordon, D. J., J. L. Probstfield, R. J. Garrison, J. D. Neaton, W. P. Castelli, J. D. Knoke, D. R. Jacobs, Jr., S. Bangdiwala, and H. A. Tyroler. 1989. High-density lipoprotein cholesterol and cardiovascular disease. Four prospective American studies. *Circulation.* **79:** 8–15.
2. Gordon, D. J., and B. M. Rifkind. 1989. High-density lipoprotein–the clinical implications of recent studies. *N. Engl. J. Med.* **321:** 1311–1316.
3. Gordon, T., W. P. Castelli, M. C. Hjortland, W. B. Kannel, and T. R. Dawber. 1977. High density lipoprotein as a protective factor against coronary heart disease. The Framingham Study. *Am. J. Med.* **62:** 707–714.
4. Miller, N. E. 1978. The evidence for the antiatherogenicity of high density lipoprotein in man. *Lipids.* **13:** 914–919.
5. Schonfeld, G., and B. Pfleger. 1974. The structure of human high density lipoprotein and the levels of apolipoprotein A-I in plasma as determined by radioimmunoassay. *J. Clin. Invest.* **54:** 236–246.
6. Schonfeld, G., J. Chen, W. F. McDonnell, and I. Jeng. 1977. Apolipoprotein A-II content of human plasma high density lipoproteins measured by radioimmunoassay. *J. Lipid Res.* **18:** 645–655.
7. Bisgaier, C. L., O. P. Sachdev, L. Megna, and R. M. Glickman. 1985. Distribution of apolipoprotein A-IV in human plasma. *J. Lipid Res.* **26:** 11–25.
8. Yao, Z., S. J. Lauer, D. A. Sanan, and S. Fazio. 1993. ApoA-IV is secreted on discrete HDL particles by the rat hepatoma cell line McA-RH7777 transfected with ApoA-IV cDNA. *Arterioscler. Thromb.* **13:** 1476–1486.
9. Shachter, N. S. 2001. Apolipoproteins C–I and C–III as important modulators of lipoprotein metabolism. *Curr. Opin. Lipidol.* **12:** 297–304.
10. Eisenberg, S. 1984. High density lipoprotein metabolism. *J. Lipid Res.* **25:** 1017–1058.
11. Blanco-Vaca, F., D. P. Via, C. Y. Yang, J. B. Massey, and H. J. Pownall. 1992. Characterization of disulfide-linked heterodimers containing apolipoprotein D in human plasma lipoproteins. *J. Lipid Res.* **33:** 1785–1796.
12. Marcel, Y. L., C. Vezina, D. Emond, and G. Suzue. 1980. Heterogeneity of human high density lipoprotein: presence of lipoproteins with and without apoE and their roles as substrates for lecithin:cholesterol acyltransferase reaction. *Proc. Natl. Acad. Sci. USA.* **77:** 2969–2973.
13. de Silva, H. V., W. D. Stuart, C. R. Duvic, J. R. Wetterau, M. J. Ray, D. G. Ferguson, H. W. Albers, W. R. Smith, and J. A. Harmony. 1990. A 70-kDa apolipoprotein designated ApoJ is a marker for subclasses of human plasma high density lipoproteins. *J. Biol. Chem.* **265:** 13240–13247.
14. Duchateau, P. N., C. R. Pullinger, R. E. Orellana, S. T. Kunitake, J. Naya-Vigne, P. M. O'Connor, M. J. Malloy, and J. P. Kane. 1997. Apolipoprotein L, a new human high density lipoprotein apolipoprotein expressed by the pancreas. Identification, cloning, characterization, and plasma distribution of apolipoprotein L. *J. Biol. Chem.* **272:** 25576–25582.
15. Kunitake, S. T., K. J. La Sala, and J. P. Kane. 1985. Apolipoprotein A-I-containing lipoproteins with pre-beta electrophoretic mobility. *J. Lipid Res.* **26:** 549–555.
16. Ishida, B. Y., J. Frolich, and C. J. Fielding. 1987. Prebeta-migrating high density lipoprotein: quantitation in normal and hyperlipidemic plasma by solid phase radioimmunoassay following electrophoretic transfer. *J. Lipid Res.* **28:** 778–786.
17. O'Connor, P. M., B. R. Zysow, S. A. Schoenhaus, B. Y. Ishida, S. T. Kunitake, J. M. Naya-Vigne, P. N. Duchateau, R. F. Redberg, S. J. Spencer, S. Mark, et al. 1998. Prebeta-1 HDL in plasma of normolipidemic individuals: influences of plasma lipoproteins, age, and gender. *J. Lipid Res.* **39:** 670–678.
18. Asztalos, B. F., C. H. Sloop, L. Wong, and P. S. Roheim. 1993. Two-dimensional electrophoresis of plasma lipoproteins: recognition of new apo A-I-containing subpopulations. *Biochim. Biophys. Acta.* **1169:** 291–300.
19. Xu, N., and B. Dahlback. 1999. A novel human apolipoprotein (apoM). *J. Biol. Chem.* **274:** 31286–31290.
20. Christoffersen, C., L. B. Nielsen, O. Axler, A. Andersson, A. H. Johnsen, and B. Dahlback. 2006. Isolation and characterization of human apolipoprotein M-containing lipoproteins. *J. Lipid Res.* **47:** 1833–1843.
21. Karlsson, H., H. Lindqvist, C. Tagesson, and M. Lindahl. 2006. Characterization of apolipoprotein M isoforms in low-density lipoprotein. *J. Proteome Res.* **5:** 2685–2690.
22. Wolfrum, C., M. N. Poy, and M. Stoffel. 2005. Apolipoprotein M is required for prebeta-HDL formation and cholesterol efflux to HDL and protects against atherosclerosis. *Nat. Med.* **11:** 418–422.
23. Mulya, A., J. Y. Lee, A. K. Gebre, M. J. Thomas, P. L. Colvin, and J. S. Parks. 2007. Minimal lipidation of pre-{beta} HDL by ABCA1 results in reduced ability to interact with ABCA1. *Arterioscler. Thromb. Vasc. Biol.* **27:** 1828–1836.
24. Wang, N., D. L. Silver, C. Thiele, and A. R. Tall. 2001. ATP-binding cassette transporter A1 (ABCA1) functions as a cholesterol efflux regulatory protein. *J. Biol. Chem.* **276:** 23742–23747.
25. Liu, L., A. E. Bortnick, M. Nickel, P. Dhanasekaran, P. V. Subbaiah, S. Lund-Katz, G. H. Rothblat, and M. C. Phillips. 2003. Effects of apolipoprotein A-I on ATP-binding cassette transporter A1-mediated efflux of macrophage phospholipid and cholesterol: formation of nascent high density lipoprotein particles. *J. Biol. Chem.* **278:** 42976–42984.
26. Duong, P. T., H. L. Collins, M. Nickel, S. Lund-Katz, G. H. Rothblat, and M. C. Phillips. 2006. Characterization of nascent HDL particles and microparticles formed by ABCA1-mediated efflux of cellular lipids to ApoA-I. *J. Lipid Res.* **47:** 832–843.

27. Krimbou, L., H. H. Hajj, S. Blain, S. Rashid, M. Denis, M. Marcil, and J. Genest. 2005. Biogenesis and speciation of nascent apoA-I-containing particles in various cell lines. *J. Lipid Res.* **46:** 1668–1677.
28. Richter, S., D. Q. Shih, E. R. Pearson, C. Wolfrum, S. S. Fajans, A. T. Hattersley, and M. Stoffel. 2003. Regulation of apolipoprotein M gene expression by MODY3 gene hepatocyte nuclear factor-1alpha: haploinsufficiency is associated with reduced serum apolipoprotein M levels. *Diabetes.* **52:** 2989–2995.
29. Timmins, J. M., J. Y. Lee, E. Boudyguina, K. D. Kluckman, L. R. Brunham, A. Mulya, A. K. Gebre, J. M. Coutinho, P. L. Colvin, T. L. Smith, et al. 2005. Targeted inactivation of hepatic Abca1 causes profound hypoalphalipoproteinemia and kidney hypercatabolism of apoA-I. *J. Clin. Invest.* **115:** 1333–1342.
30. Fujiki, Y., A. L. Hubbard, S. Fowler, and P. B. Lazarow. 1982. Isolation of intracellular membranes by means of sodium carbonate treatment: application to endoplasmic reticulum. *J. Cell Biol.* **93:** 97–102.
31. Shelness, G. S., K. C. Morris-Rogers, and M. F. Ingram. 1994. Apolipoprotein B48-membrane interactions. Absence of transmembrane localization in nonhepatic cells. *J. Biol. Chem.* **269:** 9310–9318.
32. Tall, A. R., G. G. Shipley, and D. M. Small. 1976. Conformational and thermodynamic properties of apo A-1 of human plasma high density lipoproteins. *J. Biol. Chem.* **251:** 3749–3755.
33. Tall, A. R., R. J. Deckelbaum, D. M. Small, and G. G. Shipley. 1977. Thermal behavior of human plasma high density lipoprotein. *Biochim. Biophys. Acta.* **487:** 145–153.
34. Howell, K. E., and G. E. Palade. 1982. Hepatic Golgi fractions resolved into membrane and content subfractions. *J. Cell Biol.* **92:** 822–832.
35. Christoffersen, C., M. Jauhiainen, M. Moser, B. Porse, C. Ehnholm, M. Boesl, B. Dahlback, and L. B. Nielsen. 2008. Effect of apolipoprotein M on high density lipoprotein metabolism and atherosclerosis in low density lipoprotein receptor knock-out mice. *J. Biol. Chem.* **283:** 1839–1847.
36. Ahnstrom, J., K. Faber, O. Axler, and B. Dahlback. 2007. Hydrophobic ligand binding properties of the human lipocalin apolipoprotein M. *J. Lipid Res.* **48:** 1754–1762.
37. LeCureux, L. W., F. J. Kezdy, and B. W. Wattenberg. 1994. The efficiency and kinetics of secretion of apolipoprotein A-I in hepatic and non-hepatic cells. *Atherosclerosis.* **106:** 225–233.
38. Christoffersen, C., B. Dahlback, and L. B. Nielsen. 2006. Apolipoprotein M: progress in understanding its regulation and metabolic functions. *Scand. J. Clin. Lab. Invest.* **66:** 631–637.
39. Karlin, J. B., D. J. Juhn, J. I. Starr, A. M. Scanu, and A. H. Rubenstein. 1976. Measurement of human high density lipoprotein apolipoprotein A-1 in serum by radioimmunoassay. *J. Lipid Res.* **17:** 30–37.
40. Fainaru, M., M. C. Glangeaud, and S. Eisenberg. 1975. Radioimmunoassay of human high density lipoprotein apo-protein A-1. *Biochim. Biophys. Acta.* **386:** 432–443.
41. Albers, J. J., P. W. Wahl, V. G. Cabana, W. R. Hazzard, and J. J. Hoover. 1976. Quantitation of apolipoprotein A-I of human plasma high density lipoprotein. *Metabolism.* **25:** 633–644.
42. Curry, M. D., P. Alaupovic, and C. A. Suenram. 1976. Determination of apolipoprotein A and its constitutive A-I and A-II polypeptides by separate electroimmunoassays. *Clin. Chem.* **22:** 315–322.
43. Denis, M., Y. D. Landry, and X. Zha. 2008. ATP-binding cassette A1-mediated lipidation of apolipoprotein A-I occurs at the plasma membrane and not in the endocytic compartments. *J. Biol. Chem.* **283:** 16178–16186.
44. Faulkner, L. E., S. E. Panagotopulos, J. D. Johnson, L. A. Woollett, D. Y. Hui, S. R. Witting, J. N. Maiorano, and W. S. Davidson. 2008. An analysis of the role of a retroendocytosis pathway in ABCA1-mediated cholesterol efflux from macrophages. *J. Lipid Res.* **49:** 1322–1332.
45. Vedhachalam, C., A. B. Ghering, W. S. Davidson, S. Lund-Katz, G. H. Rothblat, and M. C. Phillips. 2007. ABCA1-induced cell surface binding sites for ApoA-I. *Arterioscler. Thromb. Vasc. Biol.* **27:** 1603–1609.
46. Hassan, H. H., D. Bailey, D. Y. D. Lee, I. Iatan, A. Hafiane, I. Ruel, L. Krimbou, and J. Genest. 2008. Quantitative analysis of ABCA1-dependent compartmentalization and trafficking of apolipoprotein A-I: implications for determining cellular kinetics of nascent high density lipoprotein biogenesis. *J. Biol. Chem.* **283:** 11164–11175.
47. Lorenzi, I., A. von Eckardstein, C. Cavelier, S. Radosavljevic, and L. Rohrer. 2008. Apolipoprotein A-I but not high-density lipoproteins are internalised by RAW macrophages: roles of ATP-binding cassette transporter A1 and scavenger receptor BI. *J. Mol. Med.* **86:** 171–183.
48. Chisholm, J. W., E. R. Burleson, G. S. Shelness, and J. S. Parks. 2002. ApoA-I secretion from HepG2 cells: evidence for the secretion of both lipid-poor apoA-I and intracellularly assembled nascent HDL. *J. Lipid Res.* **43:** 36–44.
49. Maric, J., R. S. Kiss, V. Franklin, and Y. L. Marcel. 2005. Intracellular lipidation of newly synthesized apolipoprotein A-I in primary murine hepatocytes. *J. Biol. Chem.* **280:** 39942–39949.
50. Mulya, A., J. Y. Lee, A. K. Gebre, E. Y. Boudyguina, S. K. Chung, T. L. Smith, P. L. Colvin, X. C. Jiang, and J. S. Parks. 2008. Initial interaction of apoA-I with ABCA1 impacts in vivo metabolic fate of nascent HDL. *J. Lipid Res.* **49:** 2390–2401.